JOURNAL OF BACTERIOLOGY, Sept. 2004, p. 5661–5671 Vol. 186, No. 17
0021-9193/04/$08.00+0 DOI: 10.1128/JB.186.17.5661–5671.2004

Cloning and Expression of *afpA*, a Gene Encoding an Antifreeze Protein from the Arctic Plant Growth-Promoting Rhizobacterium *Pseudomonas putida* GR12-2†

Naomi Muryoi,[1] Mika Sato,[2] Shoji Kaneko,[2] Hidehisa Kawahara,[1] Hitoshi Obata,[1] Mahmoud W. F. Yaish,[3] Marilyn Griffith,[3]* and Bernard R. Glick[3]

Department of Biotechnology, Kansai University, Suita, Osaka,[1] and Ikeda Food Research Co., Ltd., Fukuyama, Hiroshima,[2] Japan, and Department of Biology, University of Waterloo, Waterloo, Ontario, Canada[3]

Received 31 January 2004/Accepted 23 May 2004

The Arctic plant growth-promoting rhizobacterium *Pseudomonas putida* GR12-2 secretes an antifreeze protein (AFP) that promotes survival at subzero temperatures. The AFP is unusual in that it also exhibits a low level of ice nucleation activity. A DNA fragment with an open reading frame encoding 473 amino acids was cloned by PCR and inverse PCR using primers designed from partial amino acid sequences of the isolated AFP. The predicted gene product, AfpA, had a molecular mass of 47.3 kDa, a pI of 3.51, and no previously known function. Although AfpA is a secreted protein, it lacked an N-terminal signal peptide and was shown by sequence analysis to have two possible secretion systems: a hemolysin-like, calcium-binding secretion domain and a type V autotransporter domain found in gram-negative bacteria. Expression of *afpA* in *Escherichia coli* yielded an intracellular 72-kDa protein modified with both sugars and lipids that exhibited lower levels of antifreeze and ice nucleation activities than the native protein. The 164-kDa AFP previously purified from *P. putida* GR12-2 was a lipoglycoprotein, and the carbohydrate was required for ice nucleation activity. Therefore, the recombinant protein may not have been properly posttranslationally modified. The AfpA sequence was most similar to cell wall-associated proteins and less similar to ice nucleation proteins (INPs). Hydropathy plots revealed that the amino acid sequence of AfpA was more hydrophobic than those of the INPs in the domain that forms the ice template, thus suggesting that AFPs and INPs interact differently with ice. To our knowledge, this is the first gene encoding a protein with both antifreeze and ice nucleation activities to be isolated and characterized.

Microorganisms are able to survive exposure to subzero temperatures, in part by modifying freezing processes to obtain nutrients and/or to prevent cellular injury. For example, some epiphytic gram-negative eubacteria from genera such as *Pseudomonas*, *Pantoea* (*Erwinia*), and *Xanthomonas* use ice nucleation proteins (INPs) to promote the growth of ice in freezing-sensitive plant tissues at temperatures as high as −2°C (48, 70). These bacterial ice nucleators are composed of 120-kDa lipoglycoproteins that form large membrane-bound aggregates (44). As a result of bacterial ice nucleation, the plants freeze during light frosts and release nutrients that fuel bacterial proliferation.

In contrast, some bacteria from permanently or seasonally frozen habitats secrete antifreeze proteins (AFPs) to inhibit the growth of external ice and promote survival (61, 76). Antifreeze proteins adsorb onto the surface of ice and lower the temperature at which it grows (14). By adsorbing onto the ice surface, AFPs also inhibit its recrystallization (43). During recrystallization, water molecules migrate from smaller ice crystals to larger ones to produce a more stable form of ice that is characterized by a minimal surface area, but these larger ice crystals are more likely to injure biological organisms. Ice recrystallization occurs more rapidly at higher subzero temperatures but is also a problem when organisms are exposed to prolonged periods of freezing (43).

Although AFPs are produced by a wide range of organisms that survive freezing, including fish, insects, plants, and fungi (10, 17, 31, 75), only 15 bacteria have been reported to exhibit antifreeze activity. These include the plant growth-promoting rhizobacterium *Pseudomonas putida* GR12-2, which was originally isolated from soil from the Canadian High Arctic (47, 61); *Rhodococcus erythropolis*, isolated from the midguts of beetle larvae (17); *Micrococcus cryophilus*, isolated from chilled sausages (17); a *Moraxella* sp. isolated from Antarctic soils (77); and an additional 11 γ- and α-proteobacteria isolated from Antarctic lakes (25). Only two bacterial AFPs have been characterized to date: a 164-kDa lipoglycoprotein from *P. putida* GR12-2 (61, 76) and a 52-kDa lipoprotein from a *Moraxella* sp. (77).

P. putida GR12-2 synthesizes and secretes its AFP into the culture medium only when grown at cold temperatures (61). The contribution of the AFP to the freezing survival of *P. putida* GR12-2 was examined by selecting freezing-sensitive mutants following transposon Tn*5* mutagenesis (41). Three of the mutants with the lowest level of freezing resistance (4 to 6% survival) also secreted the smallest amount of AFP (10 to 19% of wild-type AFP accumulation). Moreover, the de-

* Corresponding author. Mailing address: Department of Biology, University of Waterloo, 200 University Ave. West, Waterloo, Ontario N2L 3G1, Canada. Phone: (519) 888-4567. Fax: (519) 746-0614. E-mail: griffith@uwaterloo.ca.

† Supplemental material for this article may be found at http://jb.asm.org/.

creased freezing resistance of these three mutants could be partially restored by adding purified AFP to mutant cell suspensions, thus demonstrating that accumulation of AFPs is one component of the mechanism for freezing resistance in these bacteria (41).

An unusual characteristic of the AFP from *P. putida* GR12-2 is that it also displays a low level of ice nucleation activity at −10°C (76). Regardless of whether this low level of ice nucleation activity contributes to the mechanism for winter survival in this bacterium, it does raise an interesting question about the relationship between AFPs and ice nucleators. We now report for the first time in bacteria the cloning and expression of *afpA*, a gene encoding an AFP from *P. putida* GR12-2, and show that its amino acid sequence has some similarity to that of INPs from other bacteria in the domain that forms the ice template. However, this region is more hydrophobic in the AFP than in the INP, indicating that the mechanisms of interaction with ice may be different for the two proteins.

MATERIALS AND METHODS

Bacterial strain. The plant growth-promoting rhizobacterium *P. putida* GR12-2 was provided by G. Brown, Agrium Inc., Saskatoon, Saskatchewan, Canada. This bacterium was originally isolated from a soil sample from the Canadian High Arctic (47). Cells were grown at room temperature on tryptic soy broth (TSB; Difco, Detroit, Mich.) agar for 2 days, and then the plates were stored at 4°C until the bacterial colonies were required (61).

For isolation of *afpA*, a single colony of *P. putida* GR12-2 was inoculated into 5 ml of sterile TSB in a 25-ml test tube. After an overnight incubation at 25°C with shaking at 120 rpm, all of the cell culture was aseptically transferred into 3 liters of sterile TSB medium. The cells were then incubated at 5°C for 6 days with shaking at 200 rpm.

SDS-PAGE and immunoblotting. Soluble proteins were denatured and separated by analytical sodium dodecyl sulfate-polyacrylamide gel electrophoresis (SDS-PAGE) on a 10- by 10- by 0.075-cm polyacrylamide (9%, wt/vol) gel according to the method of Laemmli (46). Protein concentrations were determined by the method of Bradford (6) with bovine serum albumin as the standard. Gels were stained for protein by using Coomassie brilliant blue R-250, for carbohydrate by using periodic acid-Schiff's reagent (Sigma, St. Louis, Mo.), and for lipids by using Nile blue A as described by Xu et al. (76). In addition, gels were blotted onto a nitrocellulose membrane by using a Mini trans-blot electrophoretic transfer cell (Bio-Rad, Tokyo, Japan). Blots were first incubated overnight at 4°C in blocking buffer containing 5% (wt/vol) skim milk powder in Tris-buffered saline (TBS), pH 7.5, and then incubated with the primary antibody for 2 h at room temperature in the blocking buffer, followed by four 15-min washes in TBS plus 0.1% Tween 20. The primary antibody was affinity purified from a rabbit polyclonal antibody produced against purified 164-kDa AFP and was used at a dilution of 1:7,500 (15). After the blot was incubated with alkaline phosphatase-conjugated goat anti-rabbit immunoglobulin G (IgG) (H+L) (1:3,000; Bio-Rad), positive immunoreactions were detected by using 5-bromo-4-chloro-3-indolylphosphate (BCIP) and nitroblue tetrazolium chloride (Amersham Biosciences, Piscataway, N.J.).

Amino acid sequencing. After growth at 5°C, a 164-kDa protein with antifreeze activity was purified from the bacterial growth medium by ammonium sulfate precipitation, followed by preparative SDS-PAGE as described previously by Xu et al. (76). To obtain internal amino acid sequences, 383 μg of the purified 164-kDa protein was partially digested with 1.6 μg of trypsin (EC 3.4.21.4) (from bovine pancreas; Sigma) in 32 mM Tris-HCl, pH 8.0, at 37°C for 2 h. The AfpA fragments were separated by SDS-PAGE and blotted onto a polyvinylidene difluoride membrane by using a Bio-Rad Mini trans-blot electrophoretic cell at a constant current of 350 mA for 1.5 h. The blot was stained with 0.025% Coomassie brilliant blue R-250 in 40% methanol and destained with 50% methanol. Two major tryptic peptides were excised, and the amino acid sequences were determined at the Alberta Peptide Institute (Edmonton, Alberta, Canada) with a Hewlett-Packard G1000A/1005A protein sequencer at 10 to 25 pmol by using standard Edman chemistry with a repetitive yield of 95%.

PCR. The genomic DNA of *P. putida* GR12-2, prepared by the method of Saito and Miura (56), was used as a template for PCRs. The amino acid sequences of the N-terminal and internal tryptic peptides of the isolated AfpA (Table 1) were used to design a degenerate sense primer (S3) and an antisense primer (A2) (Table 2), and PCR was conducted in a thermal cycler (TaKaRa [Kyoto, Japan] PCR Thermal Cycler SP) by using TaKaRa LA *Taq* with proofreading activity. Amplification conditions were 29 cycles of 94°C for 40 s, 55°C for 1 min, and 72°C for 1.5 min after the initial denaturation at 94°C for 1 min. A 350-bp PCR product was obtained and cloned into the pT7Blue TA vector (Novagen, Inc., Madison, Wis.), and the insert was sequenced.

TABLE 1. Amino acid sequences of the N terminus and internal tryptic fragments of AfpA

Fragment	Sequence[a]	Position[b]	Primer
N terminus[c]	**Met-Gln-Gln-Asp-Ser-Pro-Ile**-Thr-Asn-Thr-Glu-Phe-Gln-Ser	1–14	S3
Internal A	Ala-Phe-Ile-Phe-Asp-Ser-Asn-Ala-Ser-Leu-Ala-Val-**Thr-Phe-Asp-Ala-Phe-Val-Ala**	90–108	A2
Internal B	Val-Ala-Ala-Asp-Thy-Thr-Ala-Gly-Ile-Glu-Phe-Leu-Val-Thr-Thr-Gly-Ala-Gly-Asn-Asp	117–136	

[a] Amino acid sequences used to design degenerate primers are bold faced.
[b] Positions in the amino acid sequence deduced from the gene sequence.
[c] The N-terminal sequence was previously determined by Xu et al. (76)

On the basis of the 350-bp sequence, two additional primers, B1 and B2, were designed (Table 2) and used for inverse PCR according to the method of Silver and Keerikatte (59). After independent digestions of genomic DNA with either PstI or XmaI, the DNA was self-ligated. The ligated DNA fragments were used as templates, and 30 PCR cycles, consisting of denaturation at 94°C for 1 min, annealing at 65°C for 1 min, extension at 72°C for 3 min, and a final extension at 72°C for 10 min, were used for amplification. The inverse PCR products were then cloned and sequenced. A complete sequence of *afpA* was determined by combining the sequences obtained by PCR and inverse PCR (Fig. 1A).

Construction and expression of pET3b-*afpA* in *Escherichia coli* cells. Once the complete sequence of the *afpA* gene was obtained, primers D1 and D2 (Table 2) were designed to amplify the open reading frame (ORF) by PCR using the bacterial genomic DNA as a template and TaKaRa LA *Taq*. The primers used in this PCR generated NdeI and BamHI sites at the 5′ and 3′ ends of the DNA, respectively. The reaction was performed with 25 cycles of 94°C for 1 min, 65°C for 1 min, and 72°C for 2 min. The DNA fragment containing the *afpA* structural gene was digested with NdeI and BamHI and ligated into vector pET3b (Novagen). A plasmid harboring the ORF of *afpA* inserted downstream of the T7 promoter was selected and named pET3b-*afpA*. *E. coli* BL21(DE3)/pLysS cells were transformed with the recombinant pET3b-*afpA* plasmid by the heat shock method (34).

afpA was expressed according to the instructions in the Novagen pET system manual. *E. coli* BL21(DE3)/pLysS cells carrying pET3b-*afpA* were grown in Luria-Bertani (LB) medium containing ampicillin (100 μg ml^{-1}) and chloramphenicol (34 μg ml^{-1}) at 30°C with shaking. When the optical density at 600 nm reached 0.5, 100 mM isopropyl-β-D-thiogalactopyranoside (IPTG) was added to the culture to achieve a final concentration of 0.4 mM. After a 3-h incubation at 30°C, the cells were collected by centrifugation at 3,000 × *g* for 10 min, resuspended in 50 mM Tris-HCl (pH 7.5) containing 50 mM NaCl and 1 mM EDTA,

TABLE 2. Primers used to amplify *afpA* by PCR[a]

Primer	Sequence (5′–3′)[b]
S3	ATGCARCARGAYAGYCCSATYAC
A2	GCIACIGGIGCRTCRAAVGT
B1	TGCTGGAGGTGGTCAGAAACGTT
B2	ATAGCAATGCAAGCCTGGCTGTC
D1[c]	GCCCATATGCAATACGACAGCCCAATC
D2[d]	GGATCCTAGTTACACTGCGCCGTGAAGAAC

[a] As shown in Fig. 1.
[b] I, inosine; R, A or G; S, G or C; Y, C or T; V stands for G, A, or C.
[c] The NdeI restriction site is underlined.
[d] The BamHI restriction site is underlined.

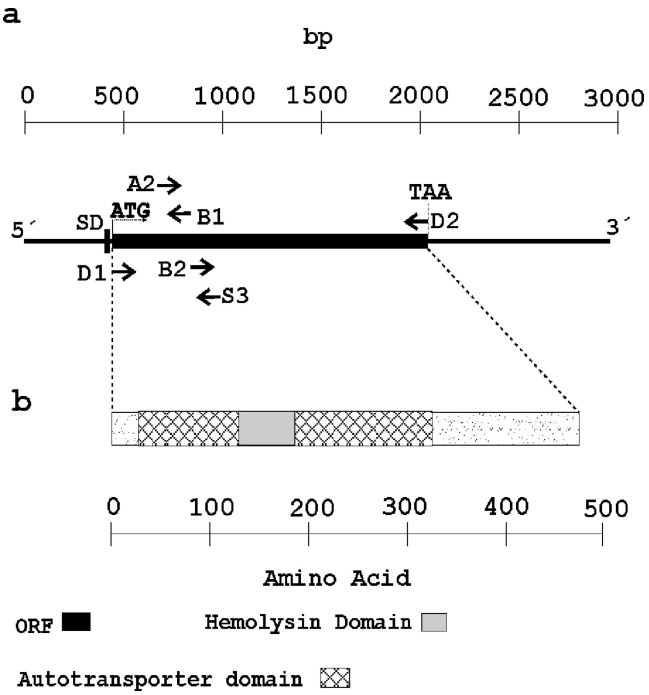

FIG. 1. (a) Schematic representation of the strategy used to isolate *afpA*. Two degenerate primers, A2 and S3, designed from the N-terminal and internal amino acid sequences of AfpA, were used to amplify a 350-bp fragment of *P. putida* GR12-2 DNA. Then the sequence of the 350-bp DNA fragment was used to amplify the flanking regions by inverse PCR with primers B1 and B2. The ORF was amplified by PCR using primers D1 and D2. (b) Map of conserved protein domains in AfpA.

and frozen at −20°C overnight. Cells were broken at 4°C by ultrasonic disintegration using a Handy Sonic model UR-20P (Tomy Seiko Co., Ltd., Tokyo, Japan) for eight pulses of 15 s each. The lysate was centrifuged at 8,000 × *g* for 10 min at 4°C, and the supernatant was used to examine soluble proteins. The recombinant AfpA was partially purified on a Toyopearl DEAE ion-exchange column (Tosoh Corp., Tokyo, Japan) preequilibrated with 20 mM sodium acetate, pH 5.5. The protein was eluted with a linear gradient of 0 to 0.2 M NaCl at a flow rate of 2 ml min^{-1} and was used for SDS-PAGE.

Assay of antifreeze activity. Antifreeze activity was assayed by observing the morphology of ice crystals grown in the presence and absence of AfpA as described by Meyer et al. (52). One microliter of protein sample was applied to the center of a temperature-controlled freezing stage (model THM 600; Linkham Scientific Instruments, Surrey, United Kingdom) on a circular glass cover. The freezing stage was fitted onto the stage of a conventional microscope and was connected to a pressurized air supply that was cooled by liquid N_2. The stage temperature was controlled by a programming unit (model TMS 90; Linkham Scientific Instruments). After sample application, the stage was heated to 20°C, cooled to −40°C at a rate of 100°C min^{-1} to freeze the sample, and then heated at the same rate to −5°C. The warming was slowed to 5°C min^{-1} to thaw the sample until only a single ice crystal was present. Subsequently, the temperature was lowered slowly in order to observe ice crystal growth. Under these conditions, high levels of antifreeze activity were indicated by a multifaceted or bipyramidal shape of the ice crystal, whereas low levels of antifreeze activity were indicated by a flat, hexagonal shape of the growing ice crystal (14). In the absence of AFPs, ice crystals were round and flat.

Measurement of ice nucleation activity. The ice-nucleating temperature was determined by using a thermoelectric cold plate (Mitsuwa model K-1; Yamamoto tekunikaru, Hirakata, Japan) as described by Vali (64). Samples included the culture broth and the soluble fraction obtained by lysing and centrifuging *E. coli* transformed with pET3b-*afpA* or pET3b and induced by IPTG. Other samples included the culture broth for *P. putida* GR12-2 that had been concentrated by ultrafiltration (Amicon; Millipore Corp., Bedford, Mass.) and intact cells of bacteria used as positive controls that were resuspended in 50 mM Tris-HCl (pH 7.5). Thirty 10-μl drops of each sample were placed on a controlled-temperature surface, which was cooled from room temperature to −20°C at a rate of 1°C min^{-1}. The temperatures at which 10% (T_{10}), 50% (T_{50}), and 90% (T_{90}) of the drops froze were recorded.

Database search and molecular modeling. The *afpA* sequence was initially characterized by conducting BLASTN and BLASTP searches (1, 2) of all GenBank nucleotide and amino acid sequence databases, followed by a specific search of the microbial genome database of *Pseudomonas* species using the National Center for Biotechnology Information (NCBI) server (http://www.ncbi.nlm.nih.gov/BLAST/). The Washington University-Blast2 (WU-Blast2) searching tool (50), accessed through the European Bioinformatics Institute server (http://www.ebi.ac.uk/blast2/), was also used to search the SWALL database for AfpA amino acid sequence homologies. In order to limit the number of sequences examined, the topcomboN value was set to 1 so as to obtain the best set of consistently high-scoring segment pairs, and sequences with expectation values (E values) of $7.7e^{-06}$ or higher were excluded from the results. The untranslated upstream region was screened for potential promoter elements by using the Neural Network Promoter Prediction service for prokaryotes (55), which is available at the Berkeley Drosophila Genome Project website (http://www.fruitfly.org/seq_tools/promoter.html), with a minimum score of 0.7 for the promoter prediction.

To identify protein domains, we used the Protein Families database (Pfam) and hidden Markov models (HMMs), available from The Sanger Institute server (4) (http://www.sanger.ac.uk/Software/Pfam/search.shtml). We searched for a possible signal peptide by using the SignalP V1.1 program (54) (Center for Biological Sequence Analysis [CBS], Technical University of Denmark [http://www.cbs.dtu.dk/services/SignalP/]). Prediction of posttranslational modification of the protein was carried out by searching for conserved motifs of possible N- and O-glucosylation and N-myristoylation sites using the CBS Prediction Servers and the ScanProsite program (23) (Swiss Institute of Bioinformatics [http://au.expasy.org/tools/scanprosite]). Mean hydropathy profiles were generated according to the general method of Kyte and Doolittle (45) by using BioEdit sequence analysis software (version 2.2; Department of Microbiology, North Carolina State University [http://www.mbio.ncsu.edu/BioEdit/bioedit.html]) with an averaging window of 13 amino acids (33). A multiple sequence alignment was constructed by using the CLUSTAL W program (62), implemented via the Bioedit program and PAM 250 protein matrices (12).

Nucleotide sequence accession number. The EMBL-GenBank-DDBJ accession number assigned to *afpA* is AJ784158

RESULTS

Cloning and characterization of the *afpA* gene. A 164-kDa protein with antifreeze activity was previously purified from *P. putida* GR12-2, and the first 14 amino acids at the N terminus were determined by Xu et al. (76). In the work reported here, two tryptic peptides from the purified 164-kDa AFP were isolated, sequenced (Table 1), and used to design primers to amplify a 350-bp fragment from *P. putida* GR12-2 genomic DNA by PCR (Table 2). The remainder of the *afpA* gene and DNA sequences both upstream and downstream of the gene were isolated by inverse PCR. The isolated DNA fragment that contained the *afpA* gene was 2,940 bp long (Fig. 1 and 2).

At the nucleotide level, a comparison of the *afpA* sequence with the EMBL database using the BLASTN program showed 65% identity, with a smallest sum probability of $5.3 \times e^{-171}$, between *afp*A and a DNA sequence of unknown function isolated from *P. putida* KT2440 in the region between bp 469 and 2940 of the *afpA* sequence. At the amino acid level, an initial BLASTP search of the genomes of *Pseudomonas* species and GenBank revealed high similarity (77 and 70%, respectively) between AfpA of *P. putida* GR12-2 and two uncharacterized proteins deduced from the full genome sequences of *Pseudomonas syringae* pv. syringae B728a and *P. putida* KT2440 (53) (Table 3). When we searched the databases on 17 January 2004, *Pseudomonas aeruginosa* PAO1, *P. putida* KT2440, and *P. syringae* pv. tomato strain DC3000 were the only *Pseudomo-*

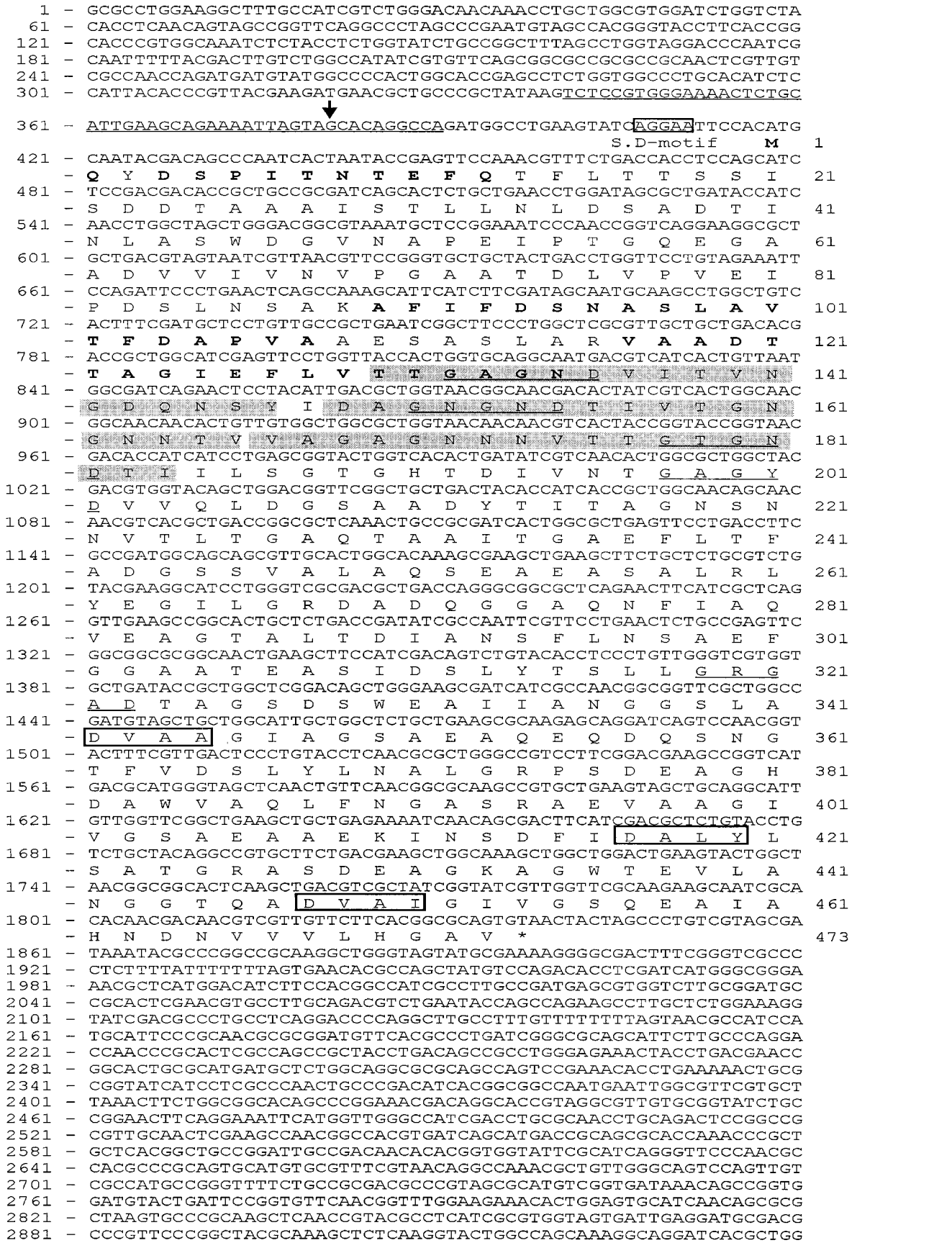
S.D-motif
M

TABLE 3. The six amino acid sequences with highest similarity to AfpA[a]

Species	Accession no.	Position	Identity (%)	Similarity (%)	E value	Reference
Pseudomonas syringae pv. syringae B728a[b]	ZP_00125445	1–473	64	77	$1e^{-121}$	
Pseudomonas putida KT2440[b]	AE016780	1–473	56	70	$1e^{-100}$	53
Caenorhabditis elegans	AF125459	111–456	28	35	$2.6e^{-12}$	72
Rhizobium leguminosarum	AY177751	129–253	35	50	$3.2e^{-12}$	71
Bradyrhizobium japonicum	AP005963	116–455	29	40	$7.1e^{-12}$	39
Rhodobacter capsulatus	AF010496	17–367	27	43	$1.3e^{-10}$	67

[a] Obtained from the microbial genome database of *Pseudomonas* spp. and from GenBank by searching with WU-Blast2 and BLASTP through the NCBI server.
[b] From the microbial genome database of *Pseudomonas* spp.

nas spp. whose genomes were completely sequenced, so we cannot exclude the presence of orthologous genes in other *Pseudomonas* spp. No homology was found between the *P. putida afpA* sequence and any DNA sequence in *P. aeruginosa* PAO1.

The possibility that multiple proteins are encoded in the *afpA* sequence was investigated by translating the nucleic acids using different ORFs. One alternative ORF was 64% identical and 78% similar to a protein isolated from *P. putida* KT2440 identified as glycosyl transferase, group 2 family (accession number NP_743949) (53). This result was interesting because some AFPs from fish and plants are homologous to carbohydrate-binding proteins (20), but we have no evidence that this ORF is expressed.

Analysis of the ORF. The predicted ORF of *afp*A encoded a protein with 473 amino acids that began 418 bp downstream from the 5′ terminus of the insert and ended with the stop codon 1,420 bp from the initiating methionine codon (Fig. 2). The predicted gene product had a molecular mass of 47.3 kDa and an isoelectric point (pI) of 3.51. The amino acid composition of the deduced product of *afpA* closely matched the amino acid composition of the previously purified AFP (76) and was enriched in alanine (17.3%) and glycine (11.0%) (Table 4).

Analysis of the 5′ untranslated region. The Neural Network Promoter Prediction service for prokaryotes (55) revealed the presence of a predicted promoter region at −27 bp from the initial methionine codon, with a possible transcription initiation site −37 bp from the initial methionine codon (Fig. 2). The neural network algorithm is thought to be a more sensitive method of predicting the Pribnow box and other sigma factor binding sites because it uses a window of 50 bp to span the transcriptional binding sites (−35 and the −10 box) in prokaryotes (55).

A predicted Shine-Dalgarno (SD) motif (58), which is an *E. coli* ribosomal binding site, was found 6 bp upstream of the methionine initiation codon (Fig. 2). However, the SD motif found in the *afpA* sequence (AGGAAT) does not match the *E. coli* SD consensus sequence of GGAGGT (52), which may have an effect on the frequency of translation initiation at this site (40).

Searching for conserved amino acid motifs. Although AfpA is known to be secreted into the culture medium, no conventional N-terminal signal peptide was found by using the SignalP signal peptide prediction tool to analyze the amino acid sequence (54). However, conserved domains in AfpA that are involved in protein secretion were identified by using the Pfam-HMMs programs (Fig. 1 and 2). The curated multiple alignments of the first database family used in this program (Pfam-A) predicted the presence of three hemolysin-type calcium-binding repeats located in the amino acid regions from residues 130 to 147, 149 to 166, and 167 to 184 of AfpA. In addition, the automatic clustering of AfpA with the second database family (Pfam-B) predicted the presence of a conserved amino acid domain located in the region between residues 27 and 319 of AfpA (Fig. 1 and 2) that is related to an autotransporter protein family that participates in the type V pathway used for secretion by gram-negative bacteria (66).

AfpA also contains five calcium-binding motifs (GXGXD) that are less conserved than the GGXGXD motif found in the cell surface proteins of other gram-negative bacteria (9, 63). Three of these putative calcium-binding sites are located within the hemolysin-like domains. Furthermore, three copies of the sequence Dhhh, where h stands for any hydrophobic residue, were found in the C terminus of AfpA (Fig. 2). These motifs, as well as the absence of an N-terminal signal sequence, are characteristic of proteins secreted via type I machinery (5, 24) and were shown to be important for recognition of secreted proteins by the translocator (18).

Prediction of posttranslational modifications. By using the CBS Prediction Servers and the ScanProsite program, the deduced amino acid sequence of *afpA* was examined for possible posttranslational modification involving glycosylation and N myristoylation. The results indicated that there are seven potential sites for N glycosylation, two sites for O glycosylation, and 20 sites for myristoylation (Fig. 3).

Expression of *afpA* in *E. coli*. To confirm that *afpA* encoded a protein with antifreeze activity, the *afpA* structural gene was

FIG. 2. Nucleotide and deduced amino acid sequences of *afpA*. Asterisk indicates translation stop codon. The predicted promoter region is underlined. A putative SD DNA motif is boxed. The predicted transcription start site within the promoter region is indicated by an arrow. The amino acid sequences of the N terminus and two internal tryptic polypeptides from the isolated native AfpA that were used to design PCR primers are boldfaced. The three sequential hemolysin-like calcium-binding regions are shaded. Five calcium-binding motifs (GXGXD) are underlined. Dhhh motifs (where "h " stands for any hydrophobic residue) that may be involved in secretion are boxed.

TABLE 4. Comparison of the amino acid composition deduced from the sequence of *afpA* and the amino acid composition of the previously purified protein[a]

Amino acid residue	Amt (mol%) in:	
	Deduced protein	Purified protein
Nonpolar		
Ala	17.26	20.5
Val	7.28	7.9
Leu	7.28	7.8
Ile	6.24	6.3
Pro	1.66	2.3
Met	0.21	0.0
Phe	2.91	2.5
Trp	0.83	ND[b]
Polar		
Gly	11.02	14.4
Ser	8.32	7.3
Thr	8.73	8.0
Cys	0.00	ND
Tyr	1.66	2.0
Asn	7.07	9.3[c]
Gln	3.33	8.1[d]
Acidic		
Asp	7.90	9.3[c]
Glu	4.78	8.1[d]
Basic		
Lys	0.62	0.7
Arg	1.66	1.9
His	0.83	0.9

[a] The amino acid composition of the previously purified protein is from reference 76.
[b] ND, not detected.
[c] Total of Asp and Asn.
[d] Total of Glu and Gln.

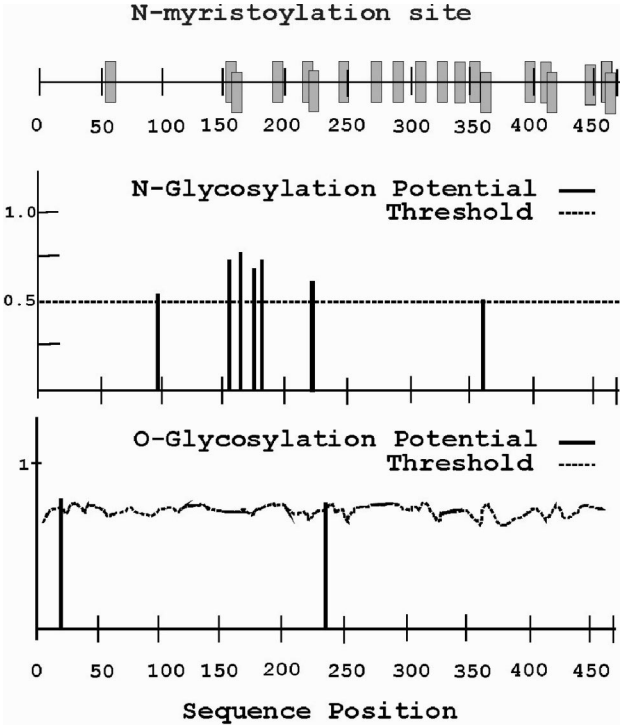

FIG. 3. Positions of potential posttranslational modifications in the AfpA amino acid sequence. Only sites that exceed the threshold value shown in each graph are likely to be modified.

inserted into the pET3b expression vector, which was then transferred into *E. coli* BL21(DE3)/pLysS cells. When these cells were grown at 30°C, a polypeptide of approximately 72 kDa, as calculated from its migration on SDS-polyacrylamide gels, was induced by IPTG (Fig. 4A). The majority of this protein accumulated in the soluble fraction of whole-cell lysates after induction by IPTG (data not shown). When immunoblots of the soluble proteins present in the lysate were probed with the affinity-purified antiserum against the 164-kDa AFP from *P. putida* GR12-2, the 72-kDa, IPTG-induced polypeptide produced in *E. coli* reacted positively (Fig. 4B). The 72-kDa polypeptide also stained positively with the periodic acid-Schiff reagent for carbohydrate and with Nile blue A for lipid (Fig. 4C).

A low level of antifreeze activity, as shown by the formation of hexagonal ice crystals, was exhibited by the soluble fraction (Fig. 4D). Although the 164-kDa AFP partially purified from the culture medium of *P. putida* GR12-2 displayed a low level of ice nucleation activity, with a T_{10} of −11°C, the extracts from *E. coli* transformed with pET3b-*afpA* had less ice nucleation activity (T_{10}, −15 to −16°C [Table 5]). The vector control culture induced by IPTG in parallel experiments had neither antifreeze activity nor ice nucleation activity (Fig. 4D; Table 5).

Comparison of AfpA with InaV. Bacterial INPs contain three domains: a central domain of repeated octapeptides comprising approximately 81% of the total sequence, a unique N-terminal domain (15%), and a unique C-terminal domain (4%) (73). Alignment of AfpA with InaV isolated from *P. syringae* (accession number AJ001086) (Table 6) (57) revealed blocks of amino acid sequence similarity with the central repeating domain of InaV that corresponds to the actual ice template (Fig. 5). However, AfpA did not contain the repeated octapeptides characteristic of INPs, and InaV did not contain the hemolysin-like, calcium-binding domains found in AfpA (Fig. 5). Of the 133 residues that were conserved between the two proteins, 30% were Gly and another 18% were Ala, which may indicate that the proteins have similar structural elements.

The mean hydrophobicity profiles of the deduced amino acid sequences of AfpA and InaV were compared in the region that corresponds to the ice template in InaV (Fig. 6). The central repeating domain of InaV exhibited a regular, repetitive pattern of hydrophilic regions. Although AfpA exhibited a similar repetitive structure, the protein was more hydrophobic in most of its sequence than the corresponding segments of InaV (Fig. 6).

DISCUSSION

A gene from *P. putida* GR12-2 encoding a protein with antifreeze activity was isolated by PCR followed by inverse PCR utilizing primers designed from the N-terminal and internal amino acid sequences of this protein. In searches conducted at the nucleic and amino acid levels, *afp*A and its product showed similarities to genes and proteins from a wide range of bacteria (Tables 3 and 6). However, the best matches had only 64 and 56% identity with deduced amino acid sequences isolated from *P. syringae* pv. syringae B728a and *P.*

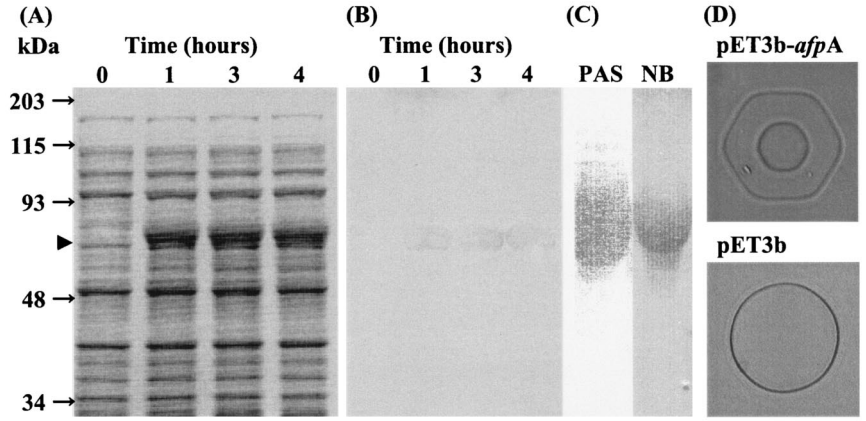

FIG. 4. Expression of pET3b-*afpA* in *E. coli* strain BL21(DE3)/pLysS analyzed by SDS-PAGE and immunoblotting. (A) Lanes 1 through 4 show the accumulation of the 72-kDa AfpA protein (arrowhead) when expression of pET3b-*afpA* was induced by IPTG and the culture was incubated at 30°C for 0, 1, 3, and 4 h, respectively. Proteins (10 μg per lane) were solubilized, separated by SDS-PAGE on a 9% (wt/vol) polyacrylamide gel, and then stained with Coomassie blue. Molecular masses of Bio-Rad protein standards are given on the left. (B) Immunoblot of a duplicate gel treated with an affinity-purified polyclonal antibody produced against the purified 164-kDa AFP. (C) AfpA was partially purified by ion-exchange chromatography, and 18 μg of protein per lane was first separated by SDS-PAGE and then stained with periodic acid-Schiff reagent (PAS) or Nile blue (NB) to show glycosylation or lipidation, respectively. (D) Antifreeze activity was assayed by observing changes in ice crystal morphology in the lysate of *E. coli* transformed with either pET3b-*afpA* or the empty pET3b vector and induced by IPTG. The crystals are shown with the basal plane (*a* axes) parallel to the plane of the page.

putida KT2440, respectively. The low identity in the deduced amino acid sequence between the industrial strain *P. putida* KT2440 and the wild-type *P. putida* GR12-2 isolated from High Arctic regions was expected, because bacteria evolve quickly under different environmental conditions, leading to intraspecific variation of their genomic sequences. Moreover, there is also large interspecific genomic variation: only 85% of the ORFs of the *P. putida* KT2440 genome have been shown to have homologues in the *P. aeruginosa* PAO1 genome (54, 60).

Secretion pathway. Analysis of the amino acid sequence of AfpA showed the absence of a conventional N-terminal signal peptide, which was not surprising given that the general export pathway is usually not sufficient to target proteins beyond the outer membrane in gram-negative bacteria (5). Pfam-B analysis showed that AfpA belongs to a family of autotransporter proteins that are secreted by the type V pathway, which was first described for the IgA1 protease (66). However, AfpA also exhibits calcium-binding and Dhhh motifs at the C terminus of the protein that are typical of the type I secretion system (3). Therefore, additional experiments are required to determine the precise secretion pathway for AfpA.

TABLE 5. Ice nucleation activities of *E. coli* transformed with pET3b-*afpA* and of various controls[a]

Strains	Ice nucleation activity (°C)		
	T_{10}	T_{50}	T_{90}
Escherichia coli pET3b-*afpA* (soluble fraction)[b]	−15.7	−18.8	−20.2
Escherichia coli pET3b-*afpA* (culture broth)[b]	−14.9	−17.6	−22.0
Escherichia coli pET3b (soluble fraction)[b]	−16.7	−18.8	−22.2
Escherichia coli pET3b (culture broth)[b]	−15.5	−17.8	−22.3
Escherichia coli JA221[c]	−13.8	−20.2	−20.7
LB medium + AMP CHL	−16.6	−19.2	−22.4
50 mM K_2HPO_4 (pH 7.0)	−19.0	−20.7	−22.2
Pseudomonas putida GR12-2 AFP[d]	−11.0	−12.0	−13.0
Pseudomonas fluorescens KUIN-1[c]	−2.6	−3.0	−3.1
Pseudomonas syringae NBRC 3310[c]	−2.1	−2.4	−2.7
Pseudomonas syringae NBRC 12656[c]	−13.8	−17.4	−21.1

[a] Negative controls included *E. coli* transformed with the empty vector and induced by IPTG, the culture broth (LB medium + AMP CHL), and the sonication buffer (50 mM K_2HPO_4 [pH 7.0]). Positive controls included *Pseudomonas* spp. known to exhibit ice nucleation activity.
[b] Soluble protein concentrations, 700 μg/ml.
[c] 1.8×10^8 cells/ml.
[d] Concentration of the partially purified AFP, 700 μg/ml.

Similar proteins. Because there were no orthologues in closely related species, we examined proteins with known functions from other bacterial species that exhibited some similarity to AfpA (Table 6). These species are all gram-negative bacteria and cyanobacteria, and most form symbiotic, mutualistic, or parasitic relationships in animal and plant host species. These proteins can be divided into three main categories: cell wall-associated proteins, nodulation proteins, and proteins with ice nucleation activity (Table 6).

The amino acid sequences of cell wall-associated proteins such as surface layer (S-layer) proteins and "repeats in structural toxins" (RTX) proteins were similar to the sequence of AfpA near the N-terminal region that contains three sequential hemolysin-like domains (Fig. 2). As explained above, these domains are found in proteins that use an unconventional secretion system in which protein export takes place without the cleavage of an N-terminal signal peptide. Like most S-layer proteins, AfpA contains no cysteine residues (26). S-layer and RTX proteins such as oscillin (36), SwmA, a cell surface protein required for motility in water (7), and AfpA all contain a combination of predicted calcium-binding motifs and N-glycosylation motifs (Fig. 3 and 4). Like AfpA, oscillin and SwmA migrate more slowly in SDS-PAGE than predicted by their molecular masses, possibly due to these posttranslational modifications that may inhibit the unfolding of the protein or the binding of SDS (51, 74).

TABLE 6. Proteins with known functions that exhibit sequence similarity to AfpA[a]

Organism	Accession no.	Position	% Identity/ % similarity	E value	Function of the protein (reference[s])
Synechococcus sp.	U48223	2–445	21/38	$2.0e^{-10}$	S-layer protein; required for bacterial motility in water (7)
Pseudomonas syringae	AJ001086	63–445	27/42	$2.9e^{-08}$	INP InaV (57)[b]
Caulobacter crescentus	AF062345	8–251	28/42	$1.4e^{-07}$	S-layer protein; serves as protector of cells from external influences (22, 26)
Rhizobium leguminosarum	X17285	135–267	28/50	$1.7e^{-07}$	Nodulation protein O (13, 19)[b]
Rhizobium meliloti	Y08703	124–293	32/49	$5.1e^{-07}$	Calcium-binding protein, directing the biosynthesis of galactoglucan (49)
Pseudomonas syringae	AF013159	7–346	26/41	$7.3e^{-07}$	INP (37)[b]
Neisseria meningitidis	L06302	128–318	30/45	$9.1e^{-07}$	RTX, iron-regulated protein FrpA; possible role in the pathogenesis of meningococcal infection (63)
Pseudomonas fluorescens	X04501	3–456	24/39	$1.6e^{-06}$	INP (69)[b]
Xanthomonas campestris	X52970	8–459	24/38	$1.7e^{-06}$	INP (78)[b]
Wolinella recta	AF010143	107–442	26/43	$2.4e^{-06}$	S-layer protein; plays a possible role in the pathogenesis of adult periodontal infection (68)
Phormidium uncinatum	AF002131	129–267	31/45	$3.3e^{-06}$	Oscillin, essential for gliding motility (36)[b]
Pseudomonas brassicacearum	AF286062	133–250	33/48	$6.6e^{-06}$	LipA; lipase-like protein involved in root infection and colonization (9)[b]
Wolinella recta	AF035192	132–449	26/39	$7.6e^{-06}$	S-layer–RTX protein; major virulence factor of periodontal pathogen (8)

[a] Results of searching by WU-Blast2 are presented in ascending order by E value.
[b] Secreted protein.

Posttranslational modifications. Most prokaryotic proteins are not modified with either carbohydrate or lipid. Among the few exceptions are the INPs, which have been found in lichens (42) and plant-associated bacteria (32) and are modified with both carbohydrate and lipid (44). Govindarajan and Lindow (27) have previously suggested that the degree of aggregation of INPs on the surfaces of ice nucleation-active bacteria is correlated with the temperature of ice nucleation. Larger aggregates of INPs can orient more water molecules into an ice crystal lattice and initiate the growth of ice at a higher subzero temperature. For example, a single INP with a molecular mass of about 150 kDa can catalyze the formation of ice at −12°C, whereas INPs modified with carbohydrates and lipids form aggregates with a molecular mass of 19,000 kDa and initiate the growth of ice at −2°C (27, 44).

The AFP isolated from *P. putida* GR12-2 has been shown to be glycosylated by positive in-gel staining with the periodic acid-Schiff reagent (76). AFPs from other organisms, including Antarctic fish (10) and the plant *Solanum dulcamara* (16), are also known to be heavily glycosylated. In addition to the predicted glycosylation sites, the AfpA amino acid sequence contains 20 potential N-myristoylation sites. AfpA produced by *P. putida* GR12-2 was also previously shown by in-gel staining to contain lipids (76). If AfpA is myristoylated, this modification may promote reversible interactions between AfpA and the membrane and/or other proteins, or it may affect the conformation of AfpA (21).

Activity of *afpA* in an *E. coli* expression system. When *afpA* was expressed in *E. coli*, the recombinant protein showed an apparent molecular mass of 72 kDa (Fig. 4), higher than that (47.3 kDa) of the predicted product of the translated *afpA* gene sequence. This difference in mass in *E. coli* can be attributed to posttranslational modification of AfpA with carbohydrates and lipids (Fig. 4). However, the antifreeze and ice nucleation activities of the 72-kDa AfpA product were lower than those observed for the native 164-kDa counterpart produced in *P. putida* GR12-2 (Fig. 4; Table 5) (76), which may be due to improper protein folding or differences in posttranslational modification, especially since Xu et al. (76) reported that ice nucleation activity decreased when the AfpA was deglycosylated experimentally. Another possibility is that highly active INPs and AFPs may be produced only at cold temperatures, as observed when *inaZ* was expressed in plants (65).

There was no change in the freezing tolerance of *E. coli* cells expressing *afpA* compared with the wild type (data not shown); however, they did not secrete AfpA into the growth medium. Accumulation of AFP in the culture broth is required to increase freezing resistance in *P. putida* GR12-2 (41). Although *P. putida* and *E. coli* are both gram-negative bacteria, the accumulation of AfpA in the cytoplasm in *E. coli* may be due to the absence of suitable membrane receptor proteins that are involved in the secretion pathway.

Interaction of AfpA with ice. INPs have a central repeat domain that is glycosylated with O-linked sugars and acts as a template to align water molecules into an ordered array, which catalyzes the crystallization of supercooled water (29). Although there is no crystal structure available for an INP, two models of secondary structure have been proposed. In one model, the largest, 48-residue repeat of InaZ was predicted to fold into three β-hairpins that interact with each other by side chains (38). In the second model, the central repeat region of InaZ was predicted to fold into a β-helix with a repetitive TXT motif on the surface of the protein that could interact with water (28). Because two insect AFPs have also been predicted to fold into β-helices with repetitive TXT motifs on the surface, Graether and Jia (28) proposed that the distinguishing feature between an AFP and an INP is the size of the domain that interacts with ice. Unlike INPs, AFPs, with a small surface

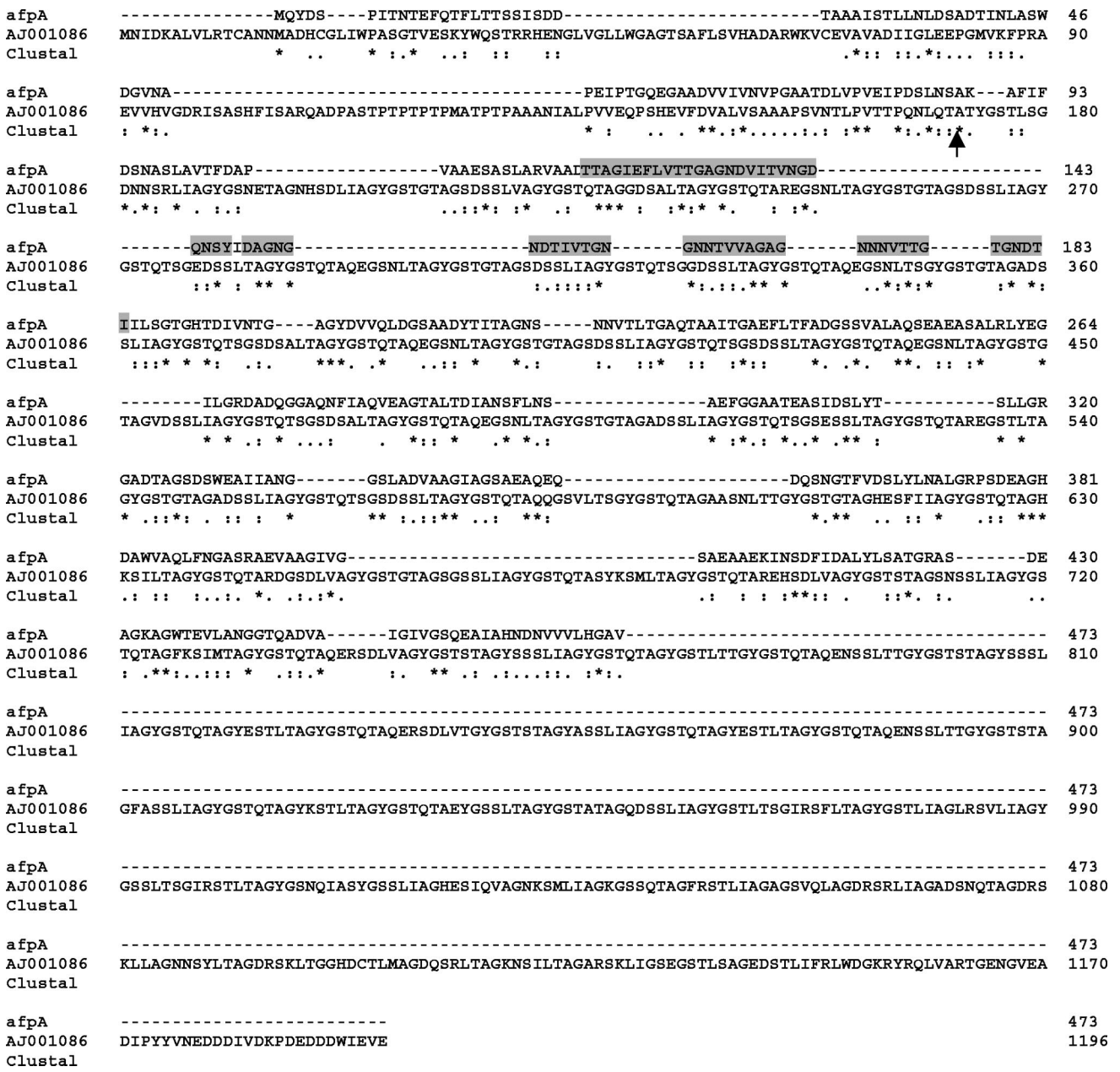

FIG. 5. Multiple alignment, produced by CLUSTAL W (62), of the deduced amino acid sequences of *P. syringae inaV* (AJ001086), encoding an ice nucleation protein, and *P. putida afpA*. Asterisks, positions at which residues are identical; colons and periods, positions at which residues belong to strongly and weakly conserved amino acid groups, respectively, according to PAM 250 protein matrices (12). Arrow indicates the beginning of the repetitive domain in InaV. The three sequential hemolysin-like domains are shaded.

area and many fewer TXT motifs, cannot assemble sufficient water molecules to form a stable ice nucleus. Instead, the water-ordering surface of the AFP could adsorb onto the surface of existing ice and inhibit its growth. However, studies using site-directed mutagenesis of the ice-binding sites of fish AFPs have now shown their ice-binding domains to be largely hydrophobic, and the adsorption of AFPs onto ice is thought to be driven entropically by desolvation of the ice face (11, 35). In these models, AFPs have a surface shape that is complementary to a face of the ice crystal lattice, and the interaction between AFPs and ice is stabilized by van der Waals contacts (11).

As shown in Fig. 6, the amino acid sequence of the ice template of InaV is quite hydrophilic, with a repetitive structure, features consistent with its role in aligning water molecules by hydrogen bonds (30). On the other hand, the amino acid sequence of AfpA is more hydrophobic than that of InaV throughout this domain. If this region corresponds to the ice-binding domain of AfpA, then the surface of AfpA that interacts with ice is more hydrophobic than that of InaV, and we can conclude that one difference between an INP and an AFP may be related to the hydrophobicity of the protein surface. Glycosylation of AfpA may make the protein more hydrophilic, resulting in the low level of ice nucleation activity observed in AfpA secreted into the medium by *P. putida* GR12-2.

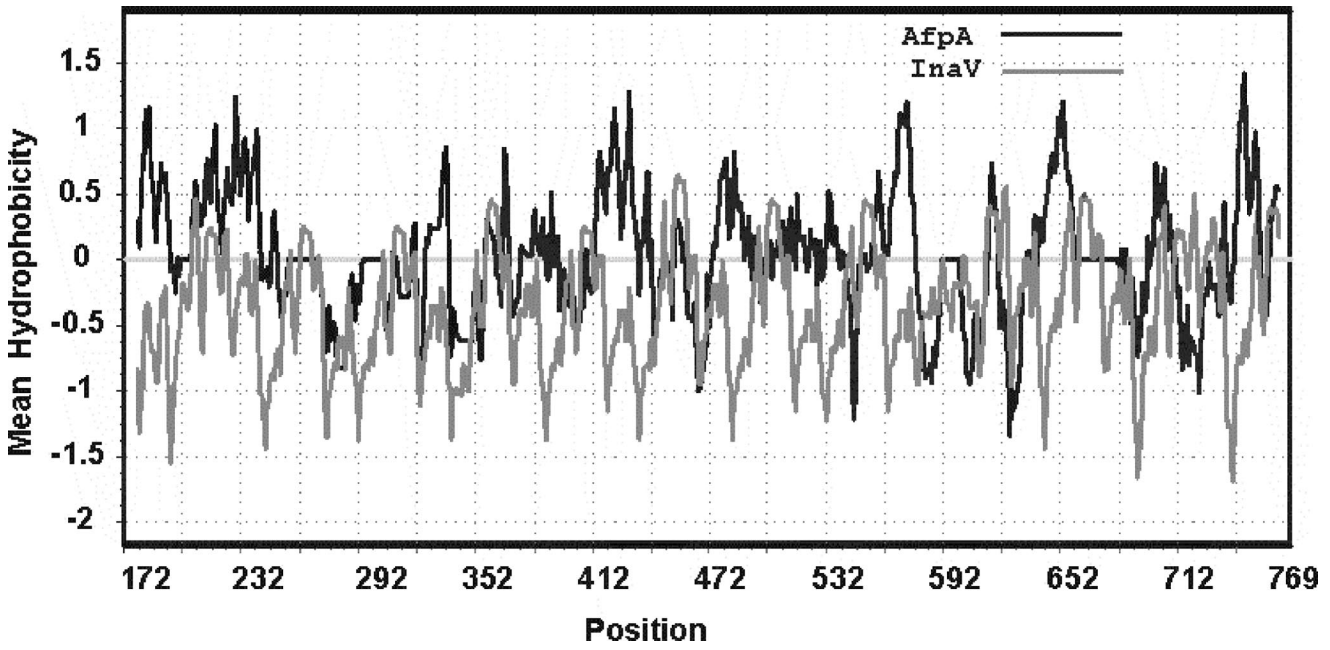

FIG. 6. Comparison of the hydropathy of the deduced amino acid sequence of the central repeat domain of *P. syringae* InaV and the homologous region of *P. putida* GR12-2 AfpA. Because the InaV sequence is much longer (1,200 amino acids) than the 473-amino-acid sequence of AfpA, only the homologous region within the central repeating domain starting at residue 172 of InaV is shown (see alignments in Fig. 5 and Fig. S1). This domain has been identified as the template for ice nucleation activity (74). A hydropathy averaging window size of 13 was used.

ACKNOWLEDGMENTS

This research was funded by the Research and Development Organization of Industry-University Cooperation from the Ministry of Education, Science, and Culture of Japan to H.K. and by Discovery Grants from the Natural Science and Engineering Research Council of Canada to M.G. and B.R.G.

REFERENCES

1. **Altschul, S. F., W. Gish, W. Miller, E. W. Myers, and D. J. Lipman.** 1990. Basic local alignment search tool. J. Mol. Biol. **215:**403–410.
2. **Altschul, S. F., T. L. Madden, A. A. Schäffer, J. Zhang, Z. Zhang, W, Miller, and D. J. Lipman.** 1997. Gapped BLAST and PSI-BLAST: a new generation of protein database search programs. Nucleic Acids Res. **25:**3389–3402.
3. **Awram, P., and J. Smit.** 1998. The *Caulobacter crescentus* paracrystalline S-layer protein is secreted by an ABC transporter (type I) secretion apparatus. J. Bacteriol. **180:**3062–3069.
4. **Bateman, A., L. Coin, R. Durbin, R. D. Finn, V. Hollich, S. Griffiths-Jones, A. Khanna, M. Marshall, S. Moxon, E. L. L. Sonnhammer, D. J. Studholme, C. Yeats, and S. R. Eddy.** 2004. The Pfam protein families database. Nucleic Acids Res. **32**(Database issue)**:**D138–D141.
5. **Binet, R., S. Létoffé, J. M. Ghigo, P. Delepelaire, and C. Wandersman.** 1997. Protein secretion by Gram-negative bacterial ABC exporters—a review. Gene **192:**7–11.
6. **Bradford, M. M.** 1976. A rapid and sensitive method for the quantitation of microgram quantities of protein utilizing the principle of protein-dye binding. Anal. Biochem. **72:**248–254.
7. **Brahamsha, B.** 1996. An abundant cell-surface polypeptide is required for swimming by the nonflagellated marine cyanobacterium *Synechococcus*. Proc. Natl. Acad. Sci. USA **93:**6504–6509.
8. **Braun, M., P. Kuhnert, J. Nicolet, A. P. Burnens, and J. Frey.** 1999. Cloning and characterization of two bistructural S-layer-RTX proteins from *Campylobacter rectus*. J. Bacteriol. **1 81:**2501–2506.
9. **Chabeaud, P., A. de Groot, W. Bitter, J. Tommassen, T. Heulin, and W. Achouak.** 2001. Phase-variable expression of an operon encoding extracellular alkaline protease, a serine protease homolog, and lipase in *Pseudomonas brassicacearum*. J. Bacteriol. **183:**2117–2120.
10. **Davies, P. L., and C. L. Hew.** 1990. Biochemistry of fish antifreeze proteins. FASEB J. **4:**2460–2468.
11. **Davies, P. L., J. Baardsnes, M. J. Kuiper, and V. K. Walker.** 2002. Structure and function of antifreeze proteins. Phil. Trans. R. Soc. Lond. B **357:**927–935.
12. **Dayhoff, M. O., R. M. Schwartz, and B. C. Orcutt.** 1978. A model of evolutionary change in proteins. Matrices for detecting distant relationships, p. 345–358. *In* M. O. Dayhoff (ed.), Atlas of protein sequence and structure, vol. 5. National Biomedical Research Foundation, Washington, D.C.
13. **de Maagd, R. A., A. H. M. Wijfjes, H. P. Spaink, J. E. Ruiz-Sainz, C. A. Wijffelman, R. J. H. Okker, and B. J. J. Lugtenberg.** 1989. *nodO*, a new *nod* gene of the *Rhizobium leguminosarum* biovar viciae sym plasmid pRL1JI, encodes a secreted protein. J. Bacteriol. **171:**6764–6770.
14. **DeVries, A. L.** 1986. Antifreeze glycopeptides and peptides: interactions with ice and water. Methods Enzymol. **127:**293–303.
15. **Donovan, R. S., C. W. Robinson, and B. R. Glick.** 2000. Optimizing the expression of a monoclonal antibody fragment under the transcriptional control of the *Escherichia coli lac* promoter. Can. J. Microbiol. **46:**532–541.
16. **Duman, J. G.** 1994. Purification and characterization of a thermal hysteresis protein from a plant, the bittersweet nightshade *Solanum dulcamara*. Biochim. Biophys. Acta **1206:**129–135.
17. **Duman, J. G., and T. M. Olsen.** 1993. Thermal hysteresis protein activity in bacteria, fungi, and phylogenetically diverse plants. Cryobiology **30:**322–328.
18. **Duong, F., A. Lazdunski, and M. Murgier.** 1996. Protein secretion by heterologous bacterial ABC-transporters: the C-terminus secretion signal of the secreted protein confers high recognition specificity. Mol. Microbiol. **21:**459–470.
19. **Economou, A., W. D. Hamilton, A. W. Johnston, and J. A. Downie.** 1990. The *Rhizobium* nodulation gene *nodO* encodes a Ca^{2+}-binding protein that is exported without N-terminal cleavage and is homologous to haemolysin and related proteins. EMBO J. **9:**349–354.
20. **Ewart, K. V., Q. Lin, and C. L. Hew.** 1999. Structure, function and evolution of antifreeze proteins. Cell. Mol. Life Sci. **55:**271–283.
21. **Farazi, T. A., G. Waksman, and J. I. Gordon.** 2001. The biology and enzymology of protein N-myristoylation. J. Biol. Chem. **276:**39501–39504.
22. **Fisher, J. A., J. K. Smit, and N. Agabian.** 1988. Transcriptional analysis of the major surface array gene of *Caulobacter crescentus*. J. Bacteriol. **170:** 4706–4713.
23. **Gattiker, A., E. Gasteiger, and A. Bairoch.** 2002. ScanProsite: a reference implementation of a PROSITE scanning tool. Appl. Bioinformatics **1:**107–108.
24. **Ghigo, J. M., and C. Wandersman.** 1994. A carboxyl-terminal four-amino acid motif is required for secretion of the metalloprotease PrtG through the *Erwinia chrysanthemi* protease secretion pathway. J. Biol. Chem. **269:**8979–8985.
25. **Gilbert, J. A., P. J. Hill, C. E. R. Dodd, and J. Laybourn-Parry.** 2004. Demonstration of antifreeze protein activity in Antarctic lake bacteria. Microbiology **150:**171–180.
26. **Gilchrist, A., J. A. Fisher, and J. K. Smit.** 1992. Nucleotide sequence analysis of the gene encoding the *Caulobacter crescentus* paracrystalline surface layer protein. Can. J. Microbiol. **38:**193–202.
27. **Govindarajan, A. J., and S. E. Lindow.** 1988. Size of bacterial ice-nucleation sites measured *in situ* by radiation inactivation analysis. Proc. Natl. Acad. Sci. USA **85:**1334–1338.

28. **Graether, S. P., and Z. Jia.** 2001. Modeling *Pseudomonas syringae* ice-nucleation protein as a β-helical protein. Biophys. J. **80:**1169–1173.
29. **Green, R. L., and G. J. Warren.** 1985. Physical and functional repetition in a bacterial ice nucleation gene. Nature **317:**645–648.
30. **Green, R. L., L. V. Corotto, and G. J. Warren.** 1988. Deletion mutagenesis of the ice nucleation gene from *Pseudomonas syringae* S203. Mol. Gen. Genet. **215:**165–172.
31. **Griffith, M., P. Ala, D. S. C. Yang, W. C. Hon, and B. A. Moffat.** 1992. Antifreeze protein produced endogenously in winter rye leaves. Plant Physiol. **100:**593–596.
32. **Gurian-Sherman, D., S. E. Lindow, and N. J. Panopoulos.** 1993. Isolation and characterization of hydroxylamine-induced mutations in the *Erwinia herbicola* ice nucleation gene that selectively reduce warm temperature ice nucleation activity. Mol. Microbiol. **9:**383–391.
33. **Hall, T. A.** 1999. BioEdit: a user-friendly biological sequence editor and analysis program for Windows 95/98/NT. Nucleic Acids Symp. Ser. **41:**95–98.
34. **Hanahan, D.** 1983. Studies on transformation of *Escherichia coli* with plasmids. J. Mol. Biol. **166:**557–580.
35. **Haymet, A. D. J., L. G. Ward, M. M. Harding, and C. A. Knight.** 1998. Valine substituted winter flounder 'antifreeze': preservation of ice growth hysteresis. FEBS Lett. **430:**301–306.
36. **Hoiczyk, E., and W. Baumeister.** 1997. Oscillin, an extracellular, Ca^{2+}-binding glycoprotein essential for the gliding motility of cyanobacteria. Mol. Microbiol. **26:**699–708.
37. **Jung, H. C., J. M. Lebeault, and J. G. Pan.** 1988. Surface display of *Zymomonas mobilis* levansucrase by using the ice-nucleation protein of *Pseudomonas syringae*. Nat. Biotechnol. **16:**576–580.
38. **Kajava, A. V., and S. E. Lindow.** 1993. A model of the 3-dimensional structure of ice nucleation proteins. J. Mol. Biol. **232:**709–717.
39. **Kaneko, T., Y. Nakamura, S. Sato, K. Minamisawa, T. Uchiumi, S. Sasamoto, A. Watanabe, K. Idesawa, M. Iriguchi, K. Kawashima, M. Kohara, M. Matsumoto, S. Shimpo, H. Tsuruoka, T. Wada, M. Yamada, and S. Tabata.** 2002. Complete genomic sequence of nitrogen-fixing symbiotic bacterium *Bradyrhizobium japonicum* USDA110. DNA Res. **9:**189–197.
40. **Karlin, S., and J. Mrazek.** 2000. Predicted highly expressed genes of diverse prokaryotic genomes. J. Bacteriol. **182:**5238–5250.
41. **Kawahara, H., J. Li, M. Griffith, and B. R. Glick.** 2001. Relationship between antifreeze protein and freezing resistance in *Pseudomonas putida* GR12–2. Curr. Microbiol. **43:**365–370.
42. **Kieft, T. L.** 1988. Ice nucleation activity in lichens. Appl. Environ. Microbiol. **54:**1678–1681.
43. **Knight, C. A., and J. G. Duman.** 1986. Inhibition of recrystallization of ice by insect thermal hysteresis proteins: a possible cryoprotective role. Cryobiology **23:**256–262.
44. **Kozloff, L. M., M. A. Turner, and F. Arellano.** 1991. Formation of bacterial membrane ice-nucleating lipoglycoprotein complexes. J. Bacteriol. **173:** 6528–6536.
45. **Kyte, J., and R. F. Doolittle.** 1982. A simple method for displaying the hydrophobic character of a protein. J. Mol. Biol. **157:**105–142.
46. **Laemmli, U. K.** 1970. Cleavage of structural proteins during the assembly of the head of bacteriophage T4. Nature **227:**680–685.
47. **Lifshitz, R., J. W. Kloepper, F. M. Scher, E. M. Tipping, and M. Laliberte.** 1986. Nitrogen-fixing pseudomonads isolated from roots of plants grown in the Canadian High Arctic. Appl. Environ. Microbiol. **51:**251–255.
48. **Lindow, S. E., D. C. Arny, C. D. Upper, and W. R. Barchet.** 1978. The role of bacterial ice nuclei in frost injury to sensitive plants, p. 249–263. *In* P. Li (ed.), Plant cold hardiness and freezing stress. Academic Press, New York, N.Y.
49. **Lloret, J., B. B. H. Wulff, J. M. Rubio, J. A. Downie, I. Bonilla, and R. Rivilla.** 1998. Exopolysaccharide II production is regulated by salt in the halotolerant strain *Rhizobium meliloti* EFB1. Appl. Environ. Microbiol. **64:**1024–1028.
50. **Lopez, R., V. Silventoinen, S. Robinson, A. Kibria, and W. Gish.** 2003. WU-Blast2 server at the European Bioinformatics Institute. Nucleic Acids Res. **31:**3795–3798.
51. **Matagune, A., B. Joris, and J. M. Frere.** 1991. Anomalous behaviour of a protein during SDS/PAGE corrected by chemical modification of carboxylic groups. Biochem. J. **280:**553–556.
52. **Meyer, K., M. Keil, and M. J. Naldrett.** 1999. A leucine-rich repeat protein of carrot that exhibits antifreeze activity. FEBS Lett. **447:**171–178.
53. **Nelson, K., I. Paulsen, C. Weinel, R. Dodson, H. Hilbert, D. Fouts, S. Gill, M. Pop, V. Martins Dos Santos, M. Holmes, L. Brinkac, M. Beanan, R. DeBoy, S. Daugherty, J. Kolonay, R. Madupu, W. Nelson, O. White, J. Peterson, H. Khouri, I. Hance, P. Lee, E. Holtzapple, D. Scanlan, K. Tran, A. Moazzez, T. Utterback, M. Rizzo, K. Lee, D. Kosack, D. Moestl, H. Wedler, J. Lauber, J. Hoheisel, M. Straetz, S. Heim, C. Kiewitz, J. Eisen, K. Timmis, A. Duesterhoft, B. Tummler, and C. Fraser.** 2002. Complete genome sequence and comparative analysis of the metabolically versatile *Pseudomonas putida* KT2440. Environ. Microbiol. **4:**799–808.
54. **Nielsen, H., J. Engelbrecht, S. Brunak, and G. von Heijne.** 1997. Identification of prokaryotic and eukaryotic signal peptides and prediction of their cleavage sites. Protein Eng. **10:**1–6.
55. **Reese, M. G.** 2001. Application of a time-delay neural network to promoter annotation in the *Drosophila melanogaster* genome. Comput. Chem. **26:**51–56.
56. **Saito, H., and K. Miura.** 1963. Preparation of transforming deoxyribonucleic acid by phenol treatment. Biochim. Biophys. Acta **72:**619–629.
57. **Schmid, D., D. Pridmore, G. Capitani, R. Battistutta, J.-R. Neeser, and A. Jann.** 1997. Molecular organisation of the ice nucleation protein InaV from *Pseudomonas syringae*. FEBS Lett. **414:**590–594.
58. **Shine, J., and L. Dalgarno.** 1974. The 3′-terminal sequence of *E. coli* 16S ribosomal RNA: complementarity to nonsense triplets and ribosome binding sites. Proc. Natl. Acad. Sci. USA **71:**1342–1346.
59. **Silver, J., and V. Keerikatte.** 1989. Novel use of polymerase chain-reaction to amplify cellular DNA adjacent to an integrated provirus. J. Virol. **63:**1924–1928.
60. **Stover, C. K., X. Q. Pham, A. L. Erwin, S. D. Mizoguchi, P. Warrener, M. J. Hickey, F. S. Brinkman, W. O. Hufnagle, D. J. Kowalik, M. Lagrou, R. L. Garber, L. Goltry, E. Tolentino, S. Westbrock-Wadman, Y. Yuan, L. L. Brody, S. N. Coulter, K. R. Folger, A. Kas, K. Larbig, R. Lim, K. Smith, D. Spencer, G. K. Wong, Z. Wu, I. T. Paulsen, J. Reizer, M. H. Saier, R. E. Hancock, S. Lory, and M. V. Olson.** 2000. Complete genome sequence of *Pseudomonas aeruginosa* PA01, an opportunistic pathogen. Nature **406:**959–964.
61. **Sun, X., M. Griffith, J. J. Pasternak, and B. R. Glick.** 1995. Low temperature growth, freezing survival and production of antifreeze protein by the plant growth promoting rhizobacterium *Pseudomonas putida* GR12–2. Can. J. Microbiol. **41:**776–784.
62. **Thompson, J. D., D. G. Higgins, and T. J. Gibson.** 1994. CLUSTAL W: improving the sensitivity of progressive multiple sequence alignment through sequence weighting, position specific gap penalties and weight matrix choice. Nucleic Acids Res. **11:**4673–4680.
63. **Thompson, S. A., L. L. Wang, A. West, and P. F. Sparling.** 1993. *Neisseria meningitidis* produces iron-regulated proteins related to the RTX family of exoproteins. J. Bacteriol. **175:**811–818.
64. **Vali, G.** 1971. Quantitative evaluation of experimental results on the heterogeneous freezing nucleation of supercooled liquids. J. Atmos. Sci. **28:**402–409.
65. **van Zee, K., D. A. Baertlein, S. E. Lindow, N. Panopoulos, and T. H. H. Chen.** 1996. Cold requirement for maximal activity of the bacterial ice nucleation protein INAZ in transgenic plants. Plant Mol. Biol. **30:**207–211.
66. **Veiga, E., E. Sugawara, H. Nikaido, V. de Lorenzo, and L. A. Fernandez.** 2002. Export of autotransported proteins proceeds through an oligomeric ring shaped by C-terminal domains. EMBO J. **21:**2122–2131.
67. **Vlcek, C., V. Paces, N. Maltsev, J. Paces, R. Haselkorn, and M. Fonstein.** 1997. Sequence of a 189-kb segment of the chromosome of *Rhodobacter capsulatus* SB1003. Proc. Natl. Acad. Sci. USA **94:**9384–9388.
68. **Wang, B., E. Kraig, and D. Kolodrubetz.** 1998. A new member of the S-layer protein family: characterization of the *crs* gene from *Campylobacter rectus*. Infect. Immun. **66:**1521–1526.
69. **Warren, G., L. Corotto, and P. Wolber.** 1986. Conserved repeats in diverged ice nucleation structural genes from two species of *Pseudomona*s. Nucleic Acids Res. **14:**8047–8060.
70. **Warren, G., and P. Wolber.** 1991. Molecular aspects of microbial ice nucleation. Mol. Microbiol. **5:**239–243.
71. **Wilkinson, A., V. Danino, F. Wisniewski-Dye, J. K. Lithgow, and J. A. Downie.** 2002. *N*-Acyl-homoserine lactone inhibition of rhizobial growth is mediated by two quorum-sensing genes that regulate plasmid transfer. J. Bacteriol. **184:**4510–4519.
72. **Wilson, R., R. Ainscough, K. Anderson, C. Baynes, M. Berks, J. Bonfield, J. Burton, M. Connell, T. Copsey, J. Cooper, A. Coulson, M. Craxton, S. Dear, Z. Du, R. Durbin, A. Favello, L. Fulton, A. Gardner, P. Green, T. Hawkins, L. Hillier, M. Jier, L. Johnston, M. Jones, J. Kershaw, J. Kirsten, N. Laister, P. Latreille, J. Lightning, C. Lloyd, A. McMurray, B. Mortimore, M. O'Callaghan, J. Parsons, C. Percy, L. Rifken, A. Roopra, D. Saunders, R. Shownkeen, N. Smaldon, A. Smith, E. Sonnhammer, R. Staden, J. Sulston, J. Thierry-Mieg, K. Thomas, M. Vaudin, K. Vaughan, R. Waterston, A. Watson, L. Weinstock, J. Wilkinson-Sproat, and P. Wohldman.** 1994. 2.2 Mb of contiguous nucleotide sequence from chromosome III of *C. elegans*. Nature **368:**32–38.
73. **Wolber, P., and G. Warren.** 1989. Bacterial ice-nucleation proteins. Trends Biochem. Sci. **14:**179–182.
74. **Wolber, P. K., C. A. Deininger, M. W. Southworth, J. Vandekerckhove, M. V. Montagu, and G. J. Warren.** 1986. Identification and purification of a bacterial ice-nucleation protein. Proc. Natl. Acad. Sci. USA **83:**7256–7260.
75. **Wu, D. W., J. G. Duman, C. C. Cheng, and F. J. Castellino.** 1991. Purification and characterization of antifreeze proteins from larvae of the beetle *Dendroides canadensis*. J. Comp. Physiol. B **161:**271–278.
76. **Xu, H., M. Griffith, C. L. Patten, and B. R. Glick.** 1998. Isolation and characterization of an antifreeze protein with ice nucleation activity from the plant growth promoting rhizobacterium *Pseudomonas putida* GR12–2. Can. J. Microbiol. **44:**64–73.
77. **Yamashita, Y., N. Nakamura, K. Omiya, J. Nishikawa, H. Kawahara, and H. Obata.** 2002. Identification of an antifreeze lipoprotein from *Moraxella* sp. of Antarctic origin. Biosci. Biotechnol. Biochem. **66:**239–247.
78. **Zhao, J. L., and C. S. Orser.** 1990. Conserved repetition in the ice nucleation gene *inaX* from *Xanthomonas campestris* pv. translucens. Mol. Gen. Genet. **223:**163–166.